

Single-Neuron Representation of Memory Strength and Recognition Confidence in Left Human Posterior Parietal Cortex

Highlights

- Neurons in human posterior parietal cortex encode declarative memory-based choices
- Memory-selective neurons preferred either novel or familiar stimuli
- Responses were modulated by memory strength as indicated by confidence
- Confidence-selective neurons signaled confidence regardless of stimulus familiarity

Authors

Ueli Rutishauser, Tyson Aflalo, Emily R. Rosario, Nader Pouratian, Richard A. Andersen

Correspondence

urut@caltech.edu

In Brief

Rutishauser, Aflalo, et al. studied the role of human posterior parietal cortex in declarative memory retrieval. They found neurons that encode memory-based familiarity and confidence for decisions in an action-independent manner, thereby revealing a role for the posterior parietal cortex in translating memories into choices.



Single-Neuron Representation of Memory Strength and Recognition Confidence in Left Human Posterior Parietal Cortex

Ueli Rutishauser,^{1,2,6,7,*} Tyson Aflalo,^{2,5,6} Emily R. Rosario,³ Nader Pouratian,⁴ and Richard A. Andersen^{2,5}

¹Department of Neurosurgery, Cedars-Sinai Medical Center, Los Angeles, CA, USA

²Division of Biology and Biological Engineering, California Institute of Technology, Pasadena, CA, USA

³Casa Colina Hospital and Centers for Healthcare, Pomona, CA, USA

⁴Department of Neurosurgery, University of California Los Angeles, Los Angeles, CA, USA

⁵Tianqiao and Chrissy Chen Brain-Machine Interface Center, California Institute of Technology, Pasadena, CA, USA

⁶These authors contributed equally

⁷Lead Contact

*Correspondence: urut@caltech.edu

<https://doi.org/10.1016/j.neuron.2017.11.029>

SUMMARY

The human posterior parietal cortex (PPC) is thought to contribute to memory retrieval, but little is known about its specific role. We recorded single PPC neurons of two human tetraplegic subjects implanted with microelectrode arrays, who performed a recognition memory task. We found two groups of neurons that signaled memory-based choices. Memory-selective neurons preferred either novel or familiar stimuli, scaled their response as a function of confidence, and signaled subjective choices regardless of truth. Confidence-selective neurons signaled confidence regardless of stimulus familiarity. Memory-selective signals appeared 553 ms after stimulus onset, but before action onset. Neurons also encoded spoken numbers, but these number-tuned neurons did not carry recognition signals. Together, this functional separation reveals action-independent coding of declarative memory-based familiarity and confidence of choices in human PPC. These data suggest that, in addition to sensory-motor integration, a function of human PPC is to utilize memory signals to make choices.

INTRODUCTION

Retrieving long-term memories to inform ongoing behavior is essential for many kinds of decisions. Examples of such decisions include determining whether you met a person before and, if so, recalling that person's name. While the processes by which perceptual decisions are made are beginning to be understood (Gold and Shadlen, 2007; Shadlen and Newsome, 2001), little is known about how long-term memories are incorporated into decisions. In macaques and rodents, neurons in the posterior parietal cortex (PPC) encode cognitive variables, such as choices and the confidence in such choices, during a

variety of perceptual and motor decision-making tasks (Andersen and Cui, 2009; Churchland et al., 2008; Gnadt and Andersen, 1988; Hanks et al., 2015; Kiani and Shadlen, 2009; Raposo et al., 2014). It presently remains unknown whether PPC neurons are also involved in making episodic memory-based choices and whether these neurons are distinct from those coding for actions.

While PPC is important for sensory-motor integration (Andersen and Buneo, 2002), a combination of imaging, lesion, and electrophysiology studies have started to reveal that the PPC also plays a role in integrating memory-based information (Gilmore et al., 2015; Sestieri et al., 2010, 2017; Wagner et al., 2005). For example, it has long been appreciated that subjects with unilateral neglect due to parietal lesions show striking spatial memory deficits (Bisiach and Luzzatti, 1978; Guariglia et al., 2005). When asked to recall a familiar scene, these patients ignore the neglected side of the imagined scene. However, the patients are able to describe the previously neglected items when asked to describe the same scene from a different imagined point of view that places the objects on their non-neglected side. Parietal lesions also cause specific recognition memory deficits: patients with PPC lesions report lower confidence in their retrieval decisions and are less likely to report the subjective experience of recollection (Hower et al., 2014; Rugg and King, 2017; Simons et al., 2010). While spatial memory deficits are most prominent after right parietal lesions, electrophysiological and neuroimaging evidence indicates that recognition memory-related signals are particularly prominent in left PPC (IPPC) (Gonzalez et al., 2015; Guerin and Miller, 2009; Wagner et al., 2005). Consequently, the IPPC is now thought to be a core component of the memory retrieval network (Olson and Berryhill, 2009; Wagner et al., 2005). Different aspects of memory retrieval modulate different areas of PPC, a degree of specialization that has given rise to multiple theories of the exact role of each in memory retrieval (Cabeza et al., 2008; Sestieri et al., 2017; Wagner et al., 2005). For example, blood-oxygen-level-dependent (BOLD)-fMRI activity in the anterior intraparietal sulcus (IPS) is larger for familiar (old) relative to novel (new) items (Hutchinson et al., 2009; Nelson et al., 2010; Sestieri et al., 2017; Uncapher and Wagner, 2009; Wimber et al., 2009; Yassa and Stark,



2008; Yonelinas et al., 2005). This activity scales proportional to memory strength for old items (Hutchinson et al., 2015) and is independent of motor and stimulus modality (Sestieri et al., 2014; Shannon and Buckner, 2004). In contrast, BOLD activity in the angular gyrus (AG) is larger for high- compared to low-confidence judgments for both new and old items (Hutchinson et al., 2015) and indicates whether an item was recollected or not (Hutchinson et al., 2014; Rugg and King, 2017; Vilberg and Rugg, 2008; Wagner et al., 2005). Dorsal superior parietal lobule (SPL) fMRI activity, on the other hand, is larger for low- compared to high-confidence judgments for both new and old items, an effect that is thought to be related to decision uncertainty (Hutchinson et al., 2014; Sestieri et al., 2010). While these extant data suggest that IPS, AG, and SPL make distinct contributions to memory retrieval, it remains unknown what signals are encoded by individual neurons in these areas.

A role of IPPC in memory retrieval is also supported by electrophysiological studies. The “parietal new/old”-evoked potential (Rugg and Curran, 2007), which differentiates new from old stimuli, has its putative source in left parietal cortex. While scalp recordings cannot differentiate between different parts of IPPC, intracranial recordings strongly support distinct roles of different parts of IPPC. Specifically, comparing gamma-band power between old and new items has revealed a striking disassociation between IPS and SPL: whereas gamma-band power is higher for old compared to new items in IPS, the opposite is the case for SPL (Gonzalez et al., 2015). In contrast, no differences of this kind were observed in AG. However, AG gamma-band activity was highest during autobiographical memory retrieval relative to other tasks (Foster et al., 2015), supporting its role in recollection. Together, this body of work supports the view that levels of neural activity in different parts of IPPC correlate with distinct aspects of episodic memory retrieval. However, little is known about the underlying mechanisms behind these changes in overall activity. In particular, it remains unknown whether IPPC neurons encoding memory-related signals are separate from those encoding action intention and execution signals. Also, the functional differences between the IPS, SPL, and AG revealed by intracranial electrocorticography (ECoG) and fMRI studies suggest that each area is specialized to encode only subsets of memory-related signals, but it remains unknown whether the same conclusion holds at the single-neuron level.

We studied the activity of individual human IPPC neurons during a recognition memory task with confidence ratings. The recognition memory-based choices in our task are thought to be made based on two sources of information: a sense of familiarity and, in addition for a subset of stimuli, recollection of associated details of the period of time when the stimulus was seen the first time. In our task, high-confidence choices are associated predominantly with recollected items whereas low-confidence items are mostly made based on familiarity alone (Wixted, 2007; Wixted et al., 2010). This feature makes our task well suited to test the neural correlates of declarative memory retrieval. Subjects were two tetraplegic subjects with chronically implanted recording arrays in IPPC, who were participating in a brain machine interface (BMI) clinical trial (Aflalo et al., 2015). Arrays were implanted within the putative human homolog of the anterior intraparietal area (AIP), an area that is part of what

is commonly labeled as anterior IPS in human fMRI studies (Hutchinson et al., 2009; Nelson et al., 2010; Sestieri et al., 2017; Uncapher and Wagner, 2009; Wimber et al., 2009; Yassa and Stark, 2008; Yonelinas et al., 2005). We found two groups of neurons whose activity was related to memory retrieval: memory-selective (MS) and confidence-selective (CS) neurons. There were two types of MS neurons, the first of which increased its firing rates for familiar stimuli and the second to novel stimuli, respectively. The strength of activity of MS neurons was modulated asymmetrically by memory strength as assessed by confidence ratings. CS neurons, on the other hand, encoded retrieval confidence symmetrically, i.e., independent of whether a stimulus was familiar or novel. During error trials, PPC neurons signaled the choice made by the subject regardless of truth, indicating that MS cells signaled choices and not ground truth. PPC cells differentiated between new and old choices approximately 550 ms after stimulus onset, a latency similar to that of the IPPC new/old event-related potential (ERP). Additional experiments confirmed that the activity of MS and CS neurons did not encode motor intentions or action signals.

RESULTS

Task and Behavior

After first memorizing 75–100 novel images, subjects performed a recognition memory test during which they rated each image as familiar (old) or novel (new). Simultaneously, they also indicated how certain they were that their choice was correct. Subjects provided verbal answers on a 1–6 confidence scale (Figure 1A; STAR Methods). Subjects provided their reply after a go cue, which appeared at an unpredictable point of time after offset of the image (Figure 1A). Across all confidence levels, subjects had good memory (Figure 1B; average area under the curve [AUC]: 0.85 ± 0.05 , \pm SD). The behavioral receiver operating characteristic (ROC) curve was asymmetric (Manns et al., 2003) as expected from a declarative memory task (Figure 1C; average slope of z-transformed ROC was 0.79 ± 0.24 , significantly less than 1, $p = 0.008$). The accuracy of retrieval decisions co-varied systematically with confidence judgments (Figures 1D–1F; mean accuracy high versus low confidence was significantly different, $p = 2.7e-13$; this difference was visible for each subject considered individually; see Figures S5A and S5B), which shows that subjects were able to assess memory strength. Decision times (DTs) varied as a function of both confidence and familiarity (Rutishauser et al., 2015): DTs were faster for high- compared to low-confidence judgments regardless of familiarity, and DTs were slower for new compared to old judgments regardless of confidence (Figure 1G; repeated-measure ANOVA, significant main effect of both familiarity $F(1,34) = 8.8$, $p = 0.0006$ and confidence $F(1,34) = 49.7$, $p < 1e-07$). Lastly, the accuracy and confidence of decisions made in response to old stimuli during recognition was independent of the position at which the same stimulus was shown when it was novel during learning (Figures 1H and 1I; repeated-measure ANOVA of binned serial position during learning; bin size 20 trials; $F(4,37) = 0.51$, $p = 0.73$ and $F(4,37) = 0.94$, $p = 0.45$ for true positive rate and confidence, respectively). This result shows that the delay between the two blocks of the task was long enough to abolish

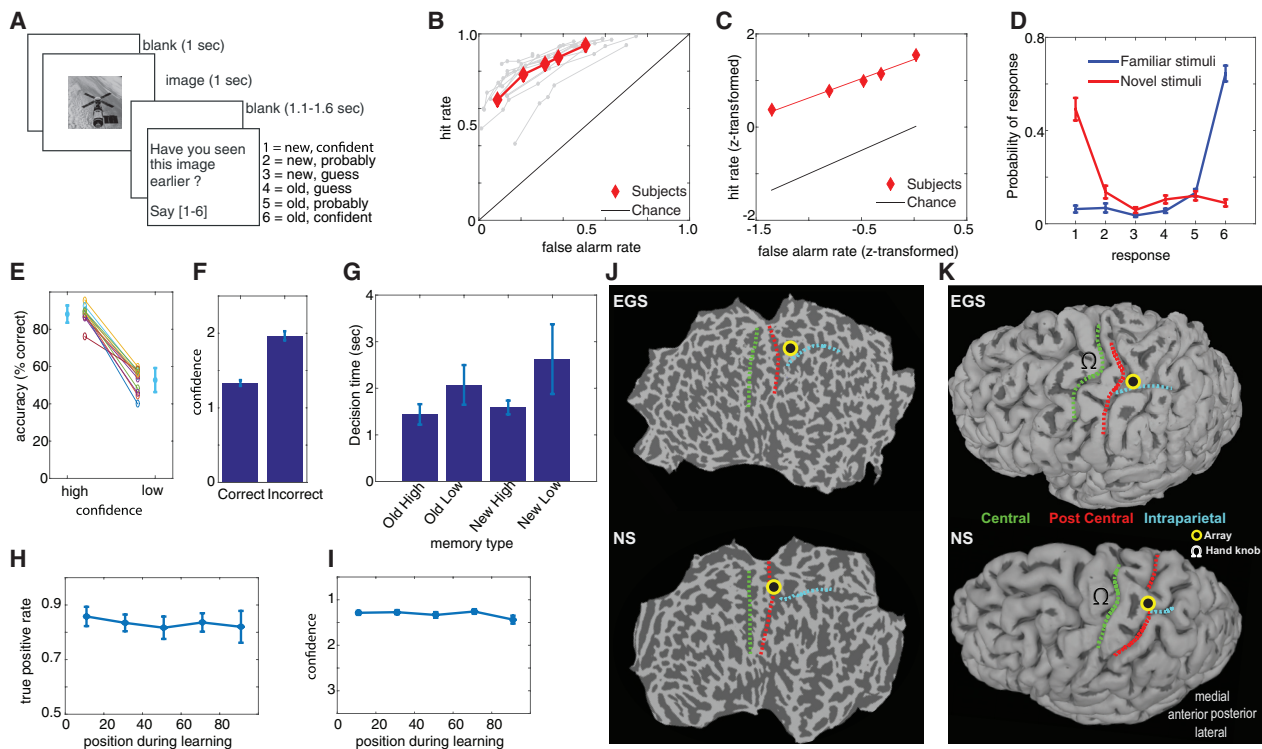


Figure 1. Task, Behavior, and Electrode Location

(A) Task.

(B) Behavioral ROC curves for each session (gray) and average (red).

(C) Z-transformed average ROC curve.

(D) Probability of response as a function of ground truth (color).

(E) Retrieval accuracy as a function of confidence.

(F) Average confidence was higher for correct versus incorrect responses.

(G) Decision time varied as a function of both familiarity (new/old) and confidence.

(H and I) True positive rate (H) and confidence (I) of responses to old stimuli during recognition was independent of serial position during learning.

(J and K) Location of recording array, illustrated using flatmaps (J) and reconstructed gray matter surfaces (K). Anatomical landmarks indicated are central sulcus (green), postcentral sulcus (red), and the intraparietal sulcus (cyan).

recency effects. Thus, different confidence ratings are not due to list position during learning. Together, the described patterns of behavior indicate that the subjects made use of medial temporal lobe (MTL)-dependent declarative memory (Kahana, 2012; Manns et al., 2003).

Electrophysiology

We recorded from a total of 1,379 individual neurons in 12 recording days from 2 patients (8 and 4 sessions, respectively; on average, 146 ± 11 and 61 ± 22 neurons recorded simultaneously, respectively; neurons recorded on different days were treated as different; mean firing rate of neurons was 2.4 ± 2.3 Hz; see Figure S1 for spike sorting metrics; see Table S1 for list of recording sessions). In both patients, the left PPC 96-channel recording array was located within the putative human homolog of the AIP (see Figures 1J and 1K). Recordings were generally stable across several hours, but not days, and we thus treated clusters identified from the same electrodes on different days as separate neurons. We use the term neuron to refer to a putative single unit throughout.

Memory- and Confidence-Selective Neurons

We first tested to what extent individual neurons were sensitive to whether a stimulus was novel or familiar. For this purpose, we used only stimuli that were correctly identified as novel or familiar by the subject (see below for analysis of error trials). Following stimulus onset, the response of 166 (12%; $p = 0.001$ versus chance, p value from bootstrap after scrambling labels, see Figure S2A; see Figures S5C and S5D for individual subjects) neurons indicated whether a stimulus was novel or familiar (Figures 2A, 2B, and 2D show examples). There were two types of such MS neurons (Figure 3A): one type increased its firing rate selectively for novel stimuli (Type 1; Figure 2A; $n = 83$, $p = 0.001$ versus chance) and the other for familiar stimuli (Type 2; Figure 2B; $n = 83$, $p = 0.001$ versus chance).

We next tested whether IPPC neurons distinguished between correct retrieval decisions made with high versus low confidence. Following stimulus onset, the response of 130 neurons (9%; $p = 0.001$ versus chance, p value from bootstrap after scrambling labels; see Figure S2B) differentiated between high- and low-confidence responses (Figure 2C shows an

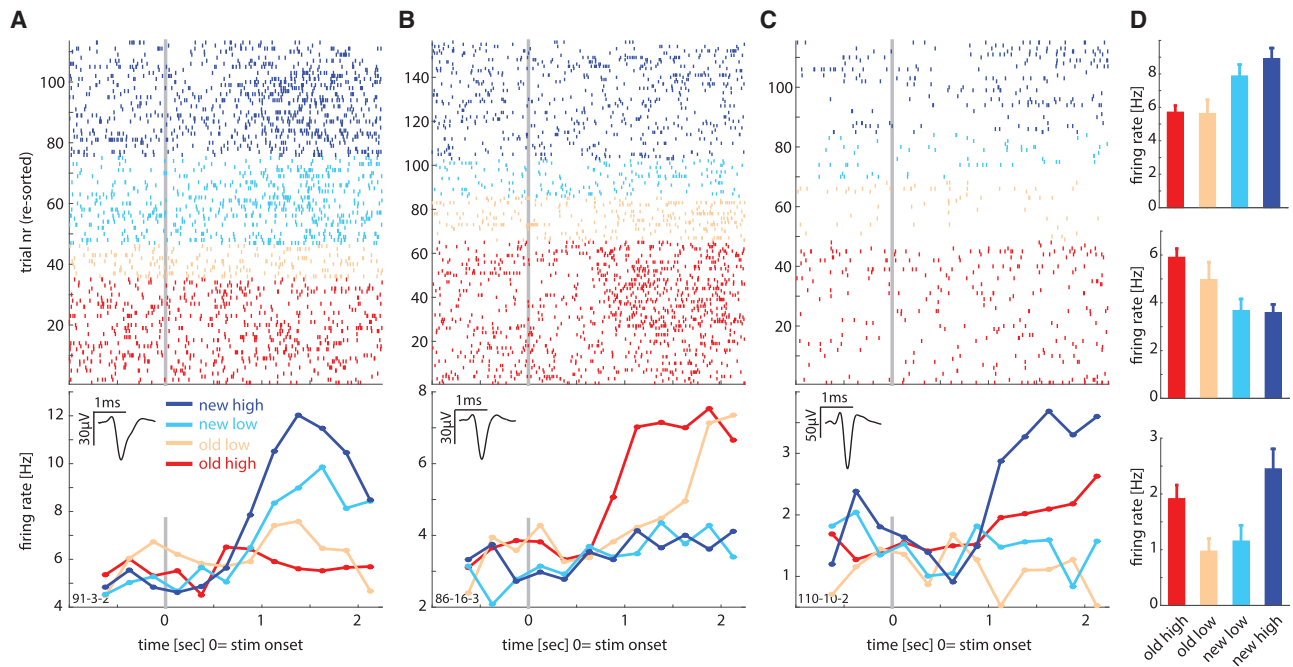


Figure 2. Examples of Individual Neurons that Carry Recognition Memory-Related Signals

(A–C) Raster (top) and PSTH (bottom) of three example neurons. Inset shows the average waveform of the neuron. Stimulus onset is at $t = 0$. Colors indicate the stimulus type (old or new) and the confidence indicated by the subject (high or low). Only trials where the subject provided the correct answer (regardless of confidence) are shown. (A) and (B) are MS cells of Type 1 (new > old) and Type 2 (old > new), respectively. Note the increase in firing rate for one, but not the other, trial type (new and old, respectively). (C) is a confidence coding cell (Type 1, high > low). (D) Average response in a 2 s window following stimulus onset for the neurons shown in (A)–(C).

example; a similar percentage qualified as CS cells in both patients, see Figure S5). Similar to the MS cells, there were two types of CS neurons (Figures 3B and 3C): one type that increased its firing rate for low-confidence decisions (Type 1; $n = 66$, $p = 0.001$ versus chance) and one that increased its firing rate for high-confidence decisions (Type 2; $n = 64$, $p = 0.001$ versus chance). Note that most CS neurons signaled retrieval confidence irrespective of whether the stimulus was old or new (Figure 3C). We thus found two types of signals relevant for recognition memory decisions that are represented by neurons in the IPPC: stimulus familiarity and retrieval confidence. We next tested whether MS cells are, in addition, also modulated by confidence.

MS Neurons Are Modulated by Memory Strength

If the response of MS cells is related to memory retrieval processes, the signal carried by MS cells should be modulated by memory strength. In contrast, if MS cell responses are purely reflective of familiarity (i.e., whether the stimulus has been seen before or not), their signal should be independent of memory strength. To evaluate these two alternatives, we next investigated whether the response of MS cells was modulated by memory strength, which here is operationalized as confidence. First, we separately averaged the confidence preference of MS cells that preferred novel (Type 1) and familiar (Type 2) items. This comparison is independent of the selection criteria used for MS cells because the selection is blind to confidence

(see STAR Methods). We found that the confidence preference for both groups was significantly larger than 0 for their preferred stimuli ($p = 0.006$ and $p = 0.004$, respectively; see Figure 3D). Thus, both types of MS cells fired more to their preferred stimulus (new or old) if the stimulus was retrieved with high compared to low confidence. Second, we confirmed this result at the single-trial level using ROC analysis. We found that the degree to which the response of an MS cell allowed an ideal observer to differentiate between new and old stimuli was significantly larger for high- compared to low-confidence trials (Figure 3E; AUC high 0.61 ± 0.06 versus AUC low 0.58 ± 0.08 , \pm SD, significantly different $p = 0.002$, paired sign test). This finding was applicable for both Type 1 and Type 2 MS cells (Figure 3F). Crucially, the response of MS cells was modulated by memory strength only for a cell's preferred stimulus, i.e., either an old or a new stimulus (Figures 4A–4C; no significant difference between non-preferred high and low confidence). For this reason, the large majority of MS cells were not selected as CS cells when using all trials (Figure S2C).

We also confirmed the sensitivity of MS cells to confidence using a different approach: we fit different generalized linear models (GLMs) separately to all neurons of either MS Type 1 or 2. We then compared the goodness of fit between the different models. A comparison between models with and without an interaction term between novelty/familiarity and confidence revealed that the model with interactions explained significantly more variance for both cell types (Figure S6A; log likelihood

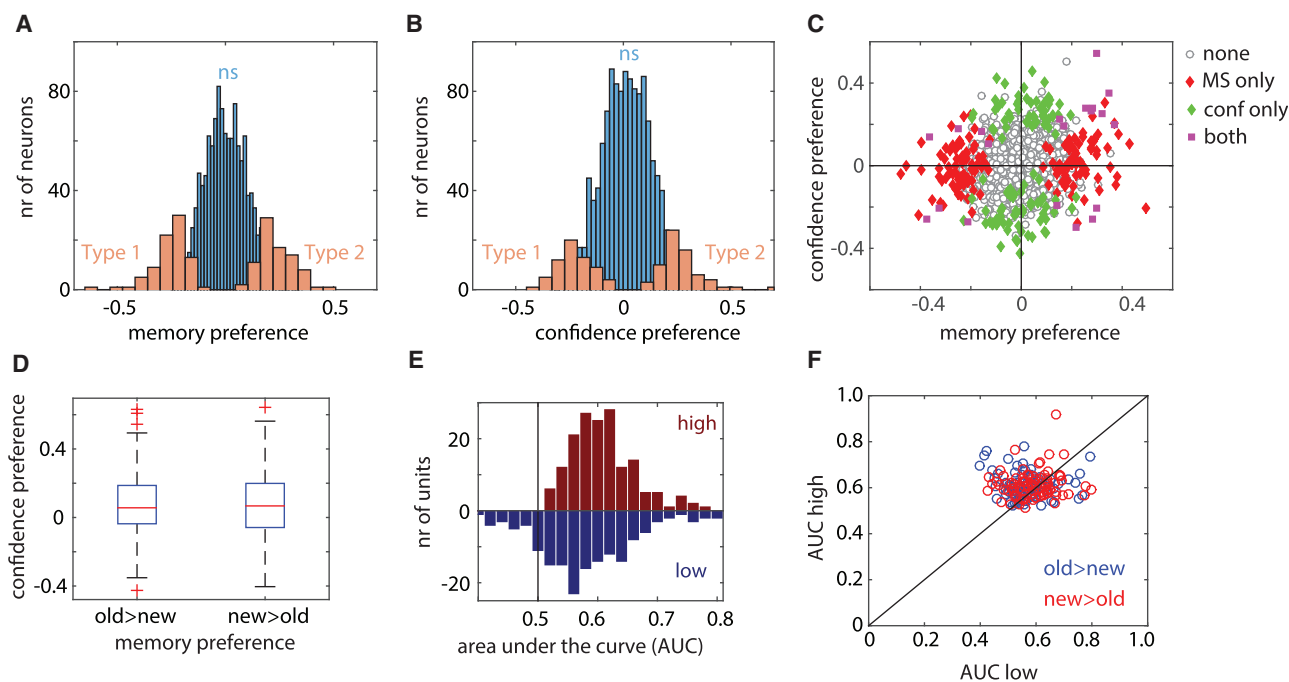


Figure 3. Population Summary of Recognition Memory Signals in PPC

(A) Distribution of memory preference across all recorded neurons. Significant MS neurons ($n = 166$) are indicated in orange and non-significant in blue. The sign of the preference indicates which stimulus each cell preferred (Type 1 versus Type 2).

(B) Distribution of confidence preference across all recorded neurons. Significant CS neurons ($n = 130$) are indicated in orange and non-significant in blue. The sign of the preference indicates which stimulus each cell preferred (Type 1 versus Type 2).

(C) Memory versus confidence preference across the population shows groups of neurons that code stimulus familiarity (red), confidence (green), or both (magenta).

(D) MS neurons have a significantly positive confidence preference ($p = 0.0057$ for old > new and $p = 0.0041$ for new > old).

(E) MS neurons provide a stronger memory signal for high- compared to low-confidence choices (AUC mirror histogram high versus low; $p = 3.02e-5$ all neurons; new > old $p = 0.014$; old > new $p = 0.00033$).

(F) AUC of high versus low confidence for each neuron, independently for MS neurons that prefer familiar (red) and novel (blue) stimuli (sign test; $p = 0.0023$, 102/164 above diagonal).

See also Figures S2, S4, and S6.

ratio-based comparison; see legend for statistics). However, critically, the interaction term was of opposite sign for MS cells of Types 1 and 2 as expected if the modulation is specific to the preferred stimulus of a cell (Figures S6B and S6C). We also tested whether DT, which co-varies with both confidence and familiarity, might explain the modulation of MS cells. However, a GLM comparison revealed that after taking into account DT differences, the effects of confidence on MS cell activity remained (see Figures S6D and S6E for details). Together, our analysis shows that MS cells are modulated by confidence, but only for their preferred stimulus.

The ROC analysis reported above is based on the same trials that were used for selection of the cells. The confidence or familiarity of the stimulus is not used for selection of MS and CS cells, respectively, making the ensuing ROC analysis independent. However, the number of trials of each type is not the same. To assess the potential effects of a larger number of high- compared to low-confidence trials, we next confirmed the ROC analysis using trials independent of those used for selection. For this, we randomly selected 50% of trials for selection and used the remainder for evaluation. We then repeated this

procedure 1,000 times (see STAR Methods). On average, 123 ± 9 MS and 124 ± 9 CS cells (\pm SD) were selected (Figures S4A and S4E), which is a smaller number of cells selected compared to when using all trials (as expected). We then computed the ROC-based metrics using the trials not used for selection. The memory preference index of MS cells was significantly negative and positive for Type 1 and Type 2 MS cells, respectively (Figure S4B; 0.08 ± 0.02 and -0.10 ± 0.02 , respectively; $p < 0.0001$ versus 0). Also, the confidence preference of MS cells for their preferred stimuli was significantly larger than 0 for both groups (see Figure S4C; $p < 0.0001$ for both, t test), and the degree to which MS cells differentiated between new and old stimuli was larger for high- compared to low-confidence trials (Figure S4D, mean AUC 0.56 ± 0.01 versus 0.52 ± 0.01 ; significantly different $p < 0.0001$, pairwise t test, mean difference 0.04 ± 0.01). Note that the mean AUC difference using all trials was comparable (0.03 ± 0.1). Similarly, for CS cells, the confidence preference was significantly positive for Type 2 (Figure S4F; 0.06 ± 0.01 , $p < 0.0001$ versus 0, t test) and significantly negative for Type 1 cells (-0.04 ± 0.03 , $p < 0.0001$ versus 0, t test). As an additional control, we repeated the same analysis

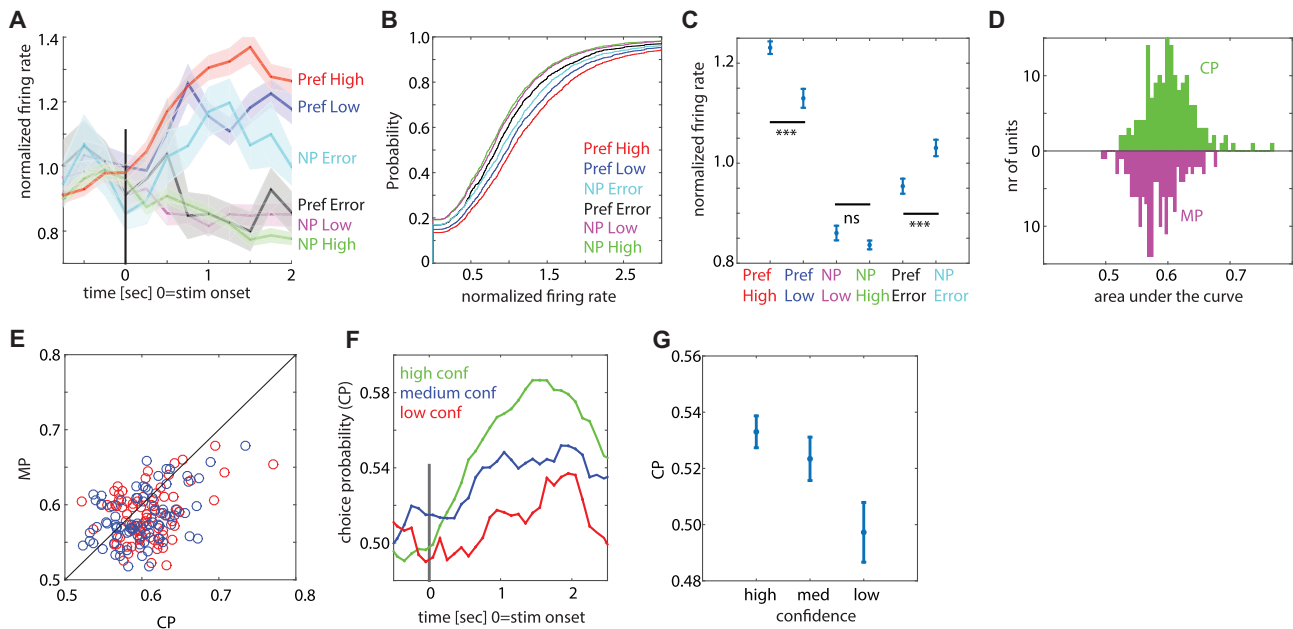


Figure 4. PPC Neurons Encode Memory-Based Choices

(A) Group PSTH of all MS neurons, pooled according to their preferred and non-preferred stimulus (Pref and NP, respectively). Tuning preference is defined according to ground truth. Note that during error trials, neurons signal according to their non-preferred stimulus (the choice). Also note modulation by confidence only for the preferred, but not non-preferred, trials.

(B and C) Single-trial analysis confirms choice coding during error trials (error non-preferred is significantly larger than error preferred $p = 9e-6$; high versus low confidence $p = 5e-5$). Shown is the full distribution (B) and the mean (C) of the single-trial response.

(D) Choice (CP) versus memory (MP) probability for all neurons.

(E) CP is significantly larger than MP for both new > old ($p = 5.9e-5$, red) and old > new ($p = 0.008$, blue) MS neurons.

(F) Time course of CP.

(G) CP varies as a function of confidence, with more reliable signaling for high confidence responses (1×3 repeated-measure ANOVA, $F = 19.8$, $p = 7.19e-9$, $n = 166$).

See also [Figure S5](#).

after randomly scrambling the trial labels (ground truth) and the responses given (behavior). This control abolished the differences between high and low confidence for both MS ([Figure S4G](#)) and CS ([Figure S4H](#)) neurons, confirming an absence of selection biases ([Figures S4G](#) and [S4H](#)). Together, this series of control analysis shows that the tuning of cells remained consistent between selection and evaluation trials and that the effects of confidence on MS cell activity remained of comparable size. Therefore, the high versus low comparison was not biased by selection.

MS Neurons Signal Memory-Based Choices

We next considered the response of MS cells during error trials, which were trials where subjects did not remember a previously shown stimulus (false negative, FN) or wrongly identified a novel stimulus as familiar (false positive, FP). If MS cells signal memory-based choices, the response during error trials should indicate the subjective choice made regardless of its truth. Alternatively, MS cells in the PPC might signal the ground truth regardless of the decision, similar to the response of hippocampal cells ([Rutishauser et al., 2008, 2015](#)). In this case, we expect the response during error trials to diverge from the decision made. To differentiate between these two hypotheses, we compare the response during error trials to that during correct

trials. We pooled the two types of MS cells according to their preferred stimulus, defined as the stimulus (new or old) resulting in the maximal response. By definition, we refer to the preferred stimulus of a cell according to ground truth (i.e., whether a stimulus is old or new regardless of behavior). Pooling the mean response of all MS cells according to these categories revealed that during error trials, MS cells increased their firing rate for error trials that corresponded to the non-preferred stimulus of the cell, but not for the preferred stimulus ([Figure 4A](#)). This pattern of response was also visible at the single-trial level: the response was stronger for non-preferred error trials compared to preferred error trials ([Figure 4B](#) shows the distribution of single-trial responses and [4C](#) the mean, $p = 9e-6$ for Pref. Error versus NP Error, Kolmogorov-Smirnov [K-S] test; this pattern of response was similar for each patient considered separately; see [Figures S5C](#) and [S5D](#)). This pattern of response shows that novelty- and familiarity-preferring cells increased their response only for FN and FP trials, respectively. We next directly assessed whether MS cell responses better predicted ground truth or choices. For this, we performed an ROC analysis to assess how well firing rate predicted either ground truth (memory probability, MP) or choices (choice probability, CP). We found that CP was significantly larger than MP ([Figures 4D](#) and [4E](#); $p = 2e-6$, paired sign test; this effect was true for both Type 1 and Type

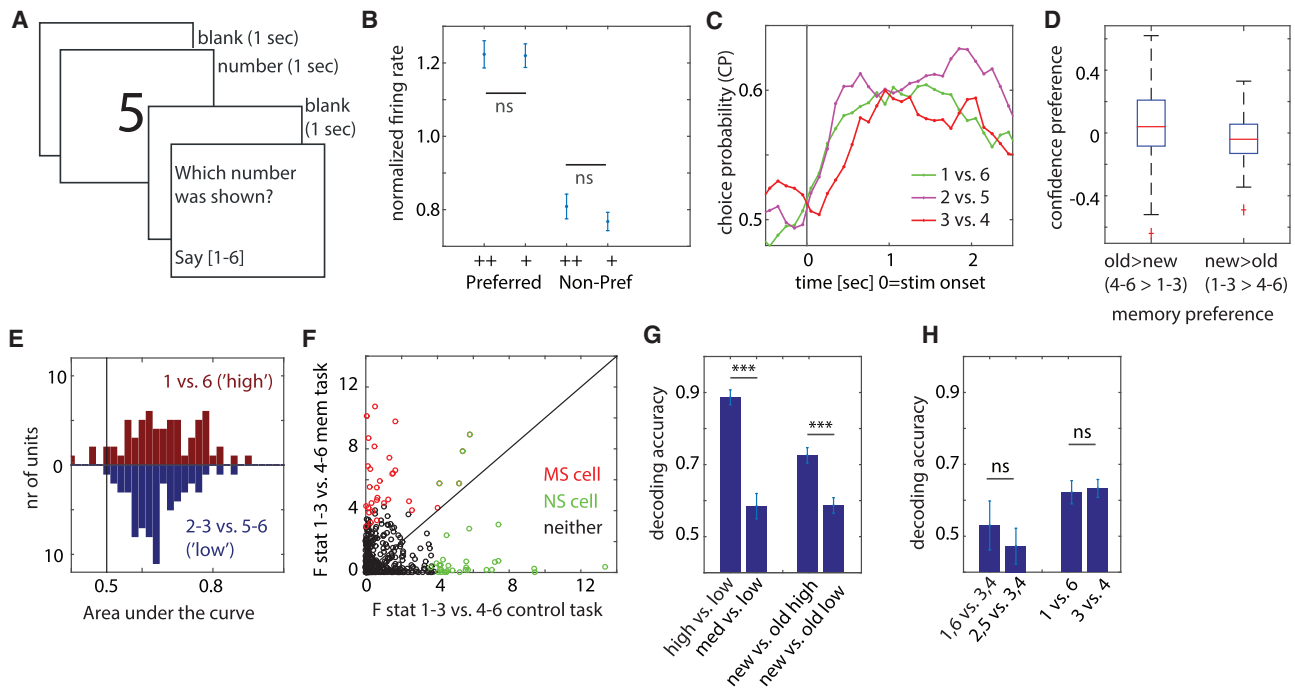


Figure 5. Neurons Encode Memory Strength and Not Action Choices

(A) Control task.

(B) Mean single-trial response shows no strength gradient ($p = 0.94$ for high [++] versus low [+] confidence indicating responses).

(C) Time course of CP does not vary as a function of confidence (1 \times 3 repeated-measure ANOVA, $F = 0.79$, $p = 0.45$, $n = 65$).

(D) Control cells have no confidence preference ($p = 0.20$ and $p = 0.23$, respectively).

(E) Control cells do not provide more information for high- compared to low-confidence decisions ($p = 0.23$).

(F) Effect size for new versus old (1–3 versus 4–6) for the control task (x axis) and the memory task (y axis). Effect sizes were not correlated ($r = -0.04$, $p = 0.82$ for NS cells; $r = 0.16$, $p = 0.36$ for MS cells; and $r = -0.02$, $p = 0.65$ for all cells recorded in both tasks), and the same neurons did not differentiate the same choices in the two tasks. Only cells recorded in both tasks are shown.

(G and H) Population decoding performance in memory (G) and control (H) task. Decoding of confidence was more accurate for high versus low confidence ($p = 9e-8$) (G). New versus old decoding was more accurate for high versus low confidence ($p = 0.0064$). Decoding performance did not differ for decoding confidence (left, $p = 0.64$) and new/old (right, $p = 0.77$) (H).

See also [Figure S3](#).

2 MS cells with $p = 5.9e-5$ and $p = 0.008$, respectively). Furthermore, CP varied systematically as a function of confidence (Figures 4F and 4G; repeated-measure 1 \times 3 ANOVA, $F(2,330) = 5.1$, $p = 0.006$). In conclusion, we found that MS cell responses signaled choices rather than ground truth. This choice signal was modulated by confidence, indicating that the response of MS cells was related to memory strength.

MS Neurons Signal Memory Strength Asymmetrically

fMRI studies have generally found that the PPC BOLD signal measured in IPS increases monotonically as a function of familiarity but that it does not differ as a function of the degree of novelty (Sestieri et al., 2014). In contrast, here we found MS cells of both types (Types 1 and 2). Critically, each MS cell was modulated by confidence (memory strength) only for its preferred, but not its non-preferred, stimulus (Figures 4A–4C; preferred high versus low $p = 5.2e-05$ whereas non-preferred high versus low was not significantly different; this difference was also visible when considering Types 1 and 2 separately, with $p = 0.018$ and $p = 0.0014$, respectively). MS cells thus coded memory strength asymmetrically because they were specialized for either novel or

familiar stimuli. Consequently, a readout mechanism for memory-based decisions would require access to both sub-types.

Memory Strength Coding Is Distinct from Action Coding

To confirm that the response of MS cells was related to memory strength, we next conducted a control experiment in which patients were shown numbers rather than images (Figure 5A). The experiment was identical in all other respects, allowing us to determine whether there are intrinsic differences in the way PPC neurons encode numbers and action plans for converting numbers into oral speech. We recorded 684 neurons across 5 recording days (in 3 of which we also performed the memory task). We then selected for cells which differentiated the numbers 1–3 from 4–6 using methods identical to those used to select for MS cells (which, identically, differentiate 1–3 from 4–6 choices in the memory task, but which in that task indicate confidence). We identified $n = 65$ (9.5%, $p = 4e-07$ versus chance) such “number-selective” (NS) cells (see Figure S3 for examples). Like for MS cells, we assigned the preferred stimulus as the category to which the NS cell had a larger response (either 1–3 or 4–6). We then proceeded to split trials according to their

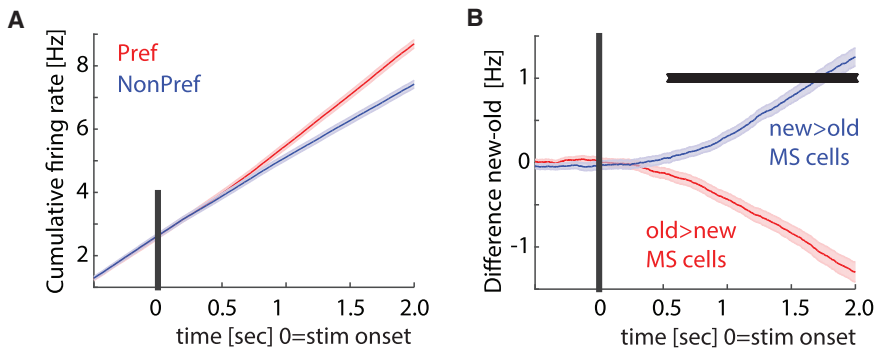


Figure 6. Latency of Memory Signal

(A) Cumulative firing rate for MS neurons.

(B) Difference of cumulative firing rate. First significant point of time was $t = 553$ ms. (Same analysis for control task: 262 ms.)

numerical response into levels of confidence, which, in this instance, were simply different numbers without further meaning of actual confidence. We then computed the same metrics we used for MS cells for the NS cells (Figures 5B–5E). This analysis revealed that NS cells did not preferentially encode the numbers we had used to indicate high or low confidence: there was no significant difference in response between high- and low-confidence-associated responses for either the preferred or non-preferred stimulus (Figure 5B; $p = 0.94$ and $p = 0.32$, respectively). Similarly, CP was high but did not differ as a function of which numbers were compared (1 versus 6, 2 versus 5, 3 versus 4; Figure 5C; repeated-measures ANOVA $F(2,128) = 0.79$, $p = 0.45$), the confidence preference index for NS neurons was not different from chance (Figure 5D; $p = 0.20$ and $p = 0.23$, respectively), and neurons did not differentiate 1 versus 6 contrasts better than 2–3 versus 4–5 contrasts (Figure 5E; $p = 0.24$). This finding shows that the preferential encoding of strong memory items was not related to the numbers used to report confidence and that the generic encoding of numbers in IPPC did not follow the pattern we observed during the memory task.

Did the same neurons signal memory strength and numbers in the two tasks? We next compared the extent to which neurons differentiated between the new and old choices (1–3 versus 4–6) in the two tasks for all neurons recorded in both tasks. This analysis revealed that the tuning of neurons in the two tasks was not related: most MS neurons that signaled memory strength did not also differentiate between the same choices (1–3 versus 4–6) during the control task and vice versa (Figure 5F; effect sizes between the two tasks were not significantly correlated; $r = 0.16$ [$p = 0.36$] and $r = -0.04$ [$p = 0.82$] for MS and NS neurons, respectively; r and p values are a Pearson correlation). Effect sizes for all recorded neurons were similarly not significantly correlated (Figure 5F; $r = -0.02$, $p = 0.65$). The representation of numbers was thus distinct from that of memory retrieval-associated processes.

Lastly, we utilized a population decoder to assess the amount of information available in groups of simultaneously recorded neurons in the two tasks (see STAR Methods). We trained one decoder to differentiate between high- and low-confidence trials and one to differentiate between new and old trials. We found that decoding performance was significantly better when the decoder had access to high- compared to low-confidence trials. This result held for both confidence decoding (Figure 5G, left; $p = 9e-8$) as well as new versus old decoding (Figure 5G, right;

actions was thus directly related to underlying memory strength but not to differences in the numbers used to communicate memory strength. Hence, the pattern of responses associated with memory strength signals could not be observed during the control task and were thus specific to memory retrieval.

Latency of Memory Strength Response

Memory-based choices take more time compared to perceptual choices, leading to the prediction that MS cells should respond relatively late after stimulus onset. Indeed, the cumulative firing rates of MS neurons (Figure 6A) first diverged between their preferred and non-preferred stimulus 553 ms after stimulus onset on average (Figure 6B). In contrast, in the control task, NS cells first differentiated between 1–3 and 4–6 responses after 262 ms following stimulus onset on average.

Population Response

Was there a difference in the average firing rate across all neurons as a function of memory strength or confidence? This question is of interest for comparison with data acquired from the same area with other methods. Averaging all MS neurons revealed little change in activity due to familiarity of the stimulus: averaging all MS neurons regardless of their tuning revealed a significant difference only due to memory strength (high versus low, paired t test, $p = 0.00087$) but not due to familiarity (new versus old, paired t test, $p = 0.55$). Similarly, averaging all recorded neurons ($n = 1,379$) shows no significant difference in the mean response between novel versus familiar or high versus low confidence trials (paired t test, $p = 0.94$ and $p = 0.20$, respectively).

DISCUSSION

The area of PPC we recorded from forms the putative human homolog of macaque AIP. In macaques, AIP is primarily a grasp area with neurons encoding both trajectory and goal information (Andersen and Buneo, 2002). Indeed, in one of our human subjects, we also documented tuning to hand shape (Klaes et al., 2015). However, neurons in human AIP also code for other goals and intentions, including whether to move the shoulder or arm in a limb-specific manner (Aflalo et al., 2015). Here, we now show that neurons in anterior IPS (where the human homolog of AIP is located; Grefkes and Fink, 2005) also encode two memory retrieval signals: familiarity of stimuli and retrieval confidence.

This finding provides direct single-neuron evidence for the long hypothesized role of the left human PPC in declarative memory retrieval (Sestieri et al., 2017; Wagner et al., 2005) and suggests that IPPC neurons signal declarative memory-based new-old choices in a manner compatible with the mnemonic accumulation hypothesis (Wagner et al., 2005).

Our data reveal that memory-based choice signals are carried by two specialized groups of MS neurons, one of which signals only new and the other only old-based choices. This result is a critical new insight different from that derived from fMRI and ECoG (Gonzalez et al., 2015; Hutchinson et al., 2014) studies, which show that BOLD and high gamma-band power ECoG activity in anterior IPS increases as a function of “oldness” of the items (Wagner et al., 2005). In contrast, in the SPL, the reverse pattern was revealed by intracranial recordings: gamma-band power was higher for novel compared to familiar items (Gonzalez et al., 2015). Here, we identified two groups of neurons in IPS that were intermixed, one preferring familiar items (MS cells Type 2) and one preferring novel items (Type 1). Within the small patch of IPS that we recorded from, we thus identified distinct neurons that each encode either familiarity- or novelty-based choices. This result disagrees with the prevailing view derived from fMRI and ECoG studies (also see Nelson et al., 2013), which suggests that, in IPS, there is a firing rate increase of old compared to new stimuli. While MS cells of Type 2 show this pattern, Type 1 MS cells show the opposite response pattern. Apart from the complex and poorly understood relation between single-neuron activity and the BOLD and gamma-band power signal, it should also be noted that our recordings were located near the border of the medial IPS and the SPL (see Figures 1J and 1K). It is therefore possible that in the more lateral IPS or more medial SPL, the proportion of tuned MS neurons is more heavily biased to old > new and new > old, respectively.

We found that the response of neurons was modulated by the confidence of the retrieval decision, a variable which does not commonly co-vary with IPS BOLD activity. Instead, it is AG (high > low) and SPL (low > high), which differentiate between different levels of retrieval confidence (Cabeza et al., 2008; Hutchinson et al., 2014). Here, we show that MS cells of both kinds are modulated by confidence (memory strength). In addition, we identified both high- and low-confidence signaling neurons, which signal confidence regardless of whether an item is new or old. We thus identified signals that, with fMRI, were previously identified only in other parts of PPC: AG for high > low and SPL for low > high. Similar to MS cells, the findings derived from single-neuron recordings thus reveal a considerably more fine-grained representation within this small patch of PPC than that suggested by fMRI. An important future experiment will be to investigate whether this discrepancy is due to complexities of the BOLD fMRI signal or rather due to the anatomical location of the recording array in a border zone between IPS and SPL. A potential experiment suggested by this result is to use multi-voxel pattern analysis of the BOLD signal from this transition area to test whether all four signals that we identified are decodable from this area.

Our patients provided their answer verbally rather than by pressing a button. Nevertheless, we found that subjects showed

all the behavioral patterns that subjects who utilize button presses exhibit. In particular, the decision time (which here is the time elapsed between question screen onset and speech onset) varied systematically as a function of familiarity and confidence as expected (Kahana, 2012). Of note, our task was not a reaction time task because subjects had to wait to provide their reply until the question screen appeared (Figure 1A). Nevertheless, we observed the expected decision time patterns, which indicates that the enforced delay was short enough to not absorb reaction time (RT) differences caused by familiarity and confidence. The same result also holds for button presses (Rutishauser et al., 2015). Hence, using verbal instead of button press responses is a valid way to measure declarative memory judgments.

Our error trial analysis revealed that PPC MS neurons signaled the choice made by the subject regardless of whether it was true or false. We found this pattern of response for both old and new decisions, which were each signaled by a specific type of MS neuron (Types 1 and 2). fMRI studies of parts of IPPC in which BOLD activity is higher for old compared to new items have similarly revealed that such activity indicates the choice made regardless of its truth (Wagner et al., 2005; Wheeler and Buckner, 2003). Here, we confirm this important distinction between choice- and ground truth-based signals.

We found that MS cells represent the strength of a memory in a continuous fashion, i.e., MS cells modulated their response as a function of confidence. This finding has two important implications: first, it supports that the signals carried by MS cells are memory related rather than action signals. Second, this type of representation is what is predicted by signal detection theories of recognition memory (Wagner et al., 2005; Wixted, 2007). These theories predict an underlying continuous decision variable that is related to the oldness of an item. In turn, the decision variable is thresholded to make a decision about whether an item is familiar and, if so, what the confidence is of the judgment. Similar familiarity signals have also been observed in IPS with BOLD-fMRI as well as ECoG (Gonzalez et al., 2015; Hutchinson et al., 2014). Here, we, in addition, identified a similarly graded signal also for novel items. Less is known about how choices about the “newness” of an item are made. For example, it is unclear whether an item is judged as new simply due to the absence of a familiarity signal. However, the presence of MS cells that signal the novelty of an item suggests that the neural substrate for new decisions involves more than the absence of a familiarity signal. Note that activity in area AG, an area of PPC that we did not record from here, has been proposed to signal whether an item was recollected or not (Nelson et al., 2010; Rugg and King, 2017; Yonelinas et al., 2005). For a recollected signal, neurons should only respond to high-confidence decisions. While we did not directly test whether subjects recollected information or not, the 1–6 confidence ratings we used are commonly used to contrast recollected (high-confidence) with not recollected (low-confidence) items. Using this approach, we found that neurons that signal high-confidence items also signaled low-confidence items (but less reliably so). It thus seems likely that MS cells were modulated by information derived from both recollection and familiarity processes. Future work is needed

to directly contrast these two different theories with respect to PPC single-neuron recordings.

The responses of some neurons in macaque PPC are tuned to numerosity (Nieder and Miller, 2004). While indirect evidence for number tuning has similarly been observed in human PPC (Dastjerdi et al., 2013; Harvey et al., 2013), no number-encoding neurons have so far been shown in humans. Here, we asked subjects to indicate their choice by verbally vocalizing a number between 1 and 6. This approach raises the question of whether the signals we reported might represent aspects of numbers rather than memory-based choices. However, the comparison with our control task revealed that MS cells did not also represent numbers. Recognition memory-based signals are expected to have specific properties, including continuity across confidence levels for either novelty or familiarity and signal strength that scales as a function of confidence (Wixted, 2007). None of these properties were present during the control task, showing that the continuous representation formed by MS cells was not present during the control task. Also, while we did identify “spoken number”-coding cells in the control task, these cells were largely distinct from those encoding memory strength because most MS cells were not also NS cells and vice versa (see Figure 5F). Together, these results show that the PPC cells we described are related to memory retrieval processes rather than a numerosity representation. In addition, these findings also show that MS cells did not signal planned actions related to the vocalizations.

In macaques, the activity of PPC neurons differentiates between different categories in tasks that require the categorization of sensory stimuli according to learned task rules (Freedman and Assad, 2006, 2016; Rishel et al., 2013). Here, we now show that the activity of human PPC neurons differentiates between novel and familiar stimuli. The concepts of “novel” and “familiar” can be regarded as categories, making our task an instance of a categorization task. However, notice that here categorization was based on an internal memory-based signal rather than the sensory input, a type of categorization that has so far not been known to involve PPC. In addition, note that the MS neurons were not a categorization signal alone because their response was also modulated by underlying memory strength as measured by confidence, but only for their preferred category. Future work will be needed to determine whether sensory- and memory-based categorization involves the same or different mechanisms and whether the types of categorization performed by PPC are domain specific or universal to all instances of categories.

In our task, differences in confidence were due to internal variability in the strength of the memory representation. Variability in the representation of the memory made decisions easier or harder, making the confidence judgment a measure of choice difficulty. In contrast, in sensory tasks, difficulty is modulated by modifying stimulus properties, making difficulty vary largely due to variation in sensory signal quality (Kiani and Shadlen, 2009). Here, in contrast, we show that PPC neurons are sensitive to internally generated variability in memory strength while keeping external signals unchanged. This meta-memory signal is the result of a significantly more complex process compared to that of assessing sensory signal strength (Metcalfe, 2008). An impor-

tant future experiment will be to determine whether the same PPC neurons can indicate both sensory- and memory-based choices and whether such neurons are modulated by both sensory- and memory-based choice difficulty. If so, this finding would indicate a common mechanism for choice difficulty. Alternatively, memory strength might be encoded in a fundamentally different manner.

How do our findings relate to the left parietal new/old ERP visible in the scalp EEG? This potential is thought to originate in left parietal cortex and differentiates new from old stimuli in the time period of 500–800 ms following stimulus onset (Rugg and Curran, 2007). The latency of PPC MS cells of, on average, 553 ms fell within this time range, indicating that MS neurons might contribute to the parietal new/old ERP. The response latency of PPC neurons was approximately 100 ms later than hippocampal MS neurons, which we previously determined had an average differential latency of 461 ms following stimulus onset in the same task (Rutishauser et al., 2015). Of note, differences in broadband gamma power between old and new stimuli have been found as early as 300 ms in IPS (Gonzalez et al., 2015). A possible explanation for the earlier onset might be that the gamma-band power primarily reflects synaptic input, whereas we measured spiking activity within PPC. An important future experiment will be to simultaneously record left parietal scalp EEG and either PPC neurons or LFP (or both) to further elucidate the contribution of individual neurons and the LFP to this ERP.

While we used visual stimuli, fMRI studies using auditory and visual stimuli in the same experiment have given rise to the proposal that the involvement of IPPC in memory retrieval is modality independent. In addition, other experiments have shown that IPPC memory retrieval activity is independent of motor output modality (eye versus hand) as well as whether a motor response is required at all (Sestieri et al., 2014; Shannon and Buckner, 2004). It will be important to confirm these observations using single-neuron studies of PPC to determine whether individual MS neurons are indeed independent of motor output and sensory input modality.

We hypothesize that PPC MS cells integrate memory-based evidence provided by the MTL (Rutishauser et al., 2015). In contrast to the PPC, individual MS cells in the MTL signal the ground truth of a memory regardless of the choice made about the memory (Rutishauser et al., 2015). These MTL cells differentiate between new and old items approximately 100 ms before PPC cells. In macaques, the presubiculum and parahippocampal gyrus provide connections to the PPC (Andersen et al., 1990; Clower et al., 2001; Insausti and Muñoz, 2001; Lavenex et al., 2002). This potential pathway might convey memory-based evidence to the PPC from the MTL. Whether these connections exist in humans and whether they target the specific area of PPC we recorded from remains to be confirmed (see Uddin et al., 2010 for functional connectivity evidence). A critical open question is how information flow from the MTL to the PPC is coordinated. Intriguingly, theta oscillations measured in PPC and MTL transiently synchronize during autobiographical memory retrieval (Foster et al., 2013), but it remains unknown whether hippocampal theta oscillations modulate PPC neurons.

STAR★METHODS

Detailed methods are provided in the online version of this paper and include the following:

- KEY RESOURCES TABLE
- CONTACT FOR REAGENT AND RESOURCE SHARING
- EXPERIMENTAL MODEL AND SUBJECT DETAILS
- METHOD DETAILS
 - Memory Task
 - Control Task
 - Electrode Placement and Electrophysiology
- QUANTIFICATION AND STATISTICAL ANALYSIS
 - Spike Detection and Sorting
 - Behavioral Analysis
 - Single-Neuron Analysis
 - Single-Neuron ROC Analysis
 - Independence of Cell Selection and ROC Analysis Bootstrap
 - Choice and Memory Probability Analysis
 - Population Analysis
 - Decoding
 - Latency Analysis
 - Bootstrap Statistics
- DATA AND SOFTWARE AVAILABILITY
- ADDITIONAL RESOURCES

SUPPLEMENTAL INFORMATION

Supplemental Information includes six figures and one table and can be found with this article online at <https://doi.org/10.1016/j.neuron.2017.11.029>.

AUTHOR CONTRIBUTIONS

U.R., T.A., and R.A.A. designed the study. U.R. and T.A. collected data and analyzed the results. U.R., T.A., and R.A.A. wrote the paper. E.R.R. provided experimental facilities and administrative assistance and coordination with Casa Colina Hospital and Centers for Healthcare. N.P. performed surgery.

ACKNOWLEDGMENTS

We thank both patients for participating in these studies and Ralph Adolphs for facilitating this collaboration through the Conte Center. This work was supported by NIH (EY015545 to R.A.A., the NIMH Conte Center at Caltech P50MH094258 to R.A.A. and U.R., and R01MH110831 to U.R.), the National Science Foundation (CAREER Award BCS-1554105 to U.R.), the T & C Chen BMI Center at Caltech, the Della Martin Foundation, and the Boswell Foundation.

Received: July 24, 2017

Revised: October 17, 2017

Accepted: November 17, 2017

Published: December 14, 2017

REFERENCES

Afialo, T., Kellis, S., Klaes, C., Lee, B., Shi, Y., Pejsa, K., Shanfield, K., Hayes-Jackson, S., Aisen, M., Heck, C., et al. (2015). Neurophysiology. Decoding motor imagery from the posterior parietal cortex of a tetraplegic human. *Science* 348, 906–910.

Andersen, R.A., and Buneo, C.A. (2002). Intentional maps in posterior parietal cortex. *Annu. Rev. Neurosci.* 25, 189–220.

Andersen, R.A., and Cui, H. (2009). Intention, action planning, and decision making in parietal-frontal circuits. *Neuron* 63, 568–583.

Andersen, R.A., Asanuma, C., Essick, G., and Siegel, R.M. (1990). Corticocortical connections of anatomically and physiologically defined subdivisions within the inferior parietal lobule. *J. Comp. Neurol.* 296, 65–113.

Bisiach, E., and Luzzatti, C. (1978). Unilateral neglect of representational space. *Cortex* 14, 129–133.

Brainard, D.H. (1997). The psychophysics toolbox. *Spat. Vis.* 10, 433–436.

Cabeza, R., Ciaramelli, E., Olson, I.R., and Moscovitch, M. (2008). The parietal cortex and episodic memory: an attentional account. *Nat. Rev. Neurosci.* 9, 613–625.

Churchland, A.K., Kiani, R., and Shadlen, M.N. (2008). Decision-making with multiple alternatives. *Nat. Neurosci.* 11, 693–702.

Clower, D.M., West, R.A., Lynch, J.C., and Strick, P.L. (2001). The inferior parietal lobule is the target of output from the superior colliculus, hippocampus, and cerebellum. *J. Neurosci.* 21, 6283–6291.

Dastjerdi, M., Ozker, M., Foster, B.L., Rangarajan, V., and Parvizi, J. (2013). Numerical processing in the human parietal cortex during experimental and natural conditions. *Nat. Commun.* 4, 2528.

Foster, B.L., Kaveh, A., Dastjerdi, M., Miller, K.J., and Parvizi, J. (2013). Human retrosplenial cortex displays transient theta phase locking with medial temporal cortex prior to activation during autobiographical memory retrieval. *J. Neurosci.* 33, 10439–10446.

Foster, B.L., Rangarajan, V., Shirer, W.R., and Parvizi, J. (2015). Intrinsic and task-dependent coupling of neuronal population activity in human parietal cortex. *Neuron* 86, 578–590.

Freedman, D.J., and Assad, J.A. (2006). Experience-dependent representation of visual categories in parietal cortex. *Nature* 443, 85–88.

Freedman, D.J., and Assad, J.A. (2016). Neuronal mechanisms of visual categorization: an abstract view on decision making. *Annu. Rev. Neurosci.* 39, 129–147.

Gilmore, A.W., Nelson, S.M., and McDermott, K.B. (2015). A parietal memory network revealed by multiple MRI methods. *Trends Cogn. Sci.* 19, 534–543.

Gnadt, J.W., and Andersen, R.A. (1988). Memory related motor planning activity in posterior parietal cortex of macaque. *Exp. Brain Res.* 70, 216–220.

Gold, J.I., and Shadlen, M.N. (2007). The neural basis of decision making. *Annu. Rev. Neurosci.* 30, 535–574.

Gonzalez, A., Hutchinson, J.B., Uncapher, M.R., Chen, J., LaRocque, K.F., Foster, B.L., Rangarajan, V., Parvizi, J., and Wagner, A.D. (2015). Electroencephalography reveals the temporal dynamics of posterior parietal cortical activity during recognition memory decisions. *Proc. Natl. Acad. Sci. USA* 112, 11066–11071.

Grefkes, C., and Fink, G.R. (2005). The functional organization of the intraparietal sulcus in humans and monkeys. *J. Anat.* 207, 3–17.

Guariglia, C., Piccardi, L., Iaria, G., Nico, D., and Pizzamiglio, L. (2005). Representational neglect and navigation in real space. *Neuropsychologia* 43, 1138–1143.

Guerin, S.A., and Miller, M.B. (2009). Lateralization of the parietal old/new effect: an event-related fMRI study comparing recognition memory for words and faces. *Neuroimage* 44, 232–242.

Hanks, T.D., Kopec, C.D., Brunton, B.W., Duan, C.A., Erlich, J.C., and Brody, C.D. (2015). Distinct relationships of parietal and prefrontal cortices to evidence accumulation. *Nature* 520, 220–223.

Harris, K.D., Henze, D.A., Csicsvari, J., Hirase, H., and Buzsáki, G. (2000). Accuracy of tetrode spike separation as determined by simultaneous intracellular and extracellular measurements. *J. Neurophysiol.* 84, 401–414.

Harvey, B.M., Klein, B.P., Petridou, N., and Dumoulin, S.O. (2013). Topographic representation of numerosity in the human parietal cortex. *Science* 341, 1123–1126.

Hower, K.H., Wixted, J., Berryhill, M.E., and Olson, I.R. (2014). Impaired perception of mnemonic oldness, but not mnemonic newness, after parietal lobe damage. *Neuropsychologia* 56, 409–417.

- Hutchinson, J.B., Uncapher, M.R., and Wagner, A.D. (2009). Posterior parietal cortex and episodic retrieval: convergent and divergent effects of attention and memory. *Learn. Mem.* *16*, 343–356.
- Hutchinson, J.B., Uncapher, M.R., Weiner, K.S., Bressler, D.W., Silver, M.A., Preston, A.R., and Wagner, A.D. (2014). Functional heterogeneity in posterior parietal cortex across attention and episodic memory retrieval. *Cereb. Cortex* *24*, 49–66.
- Hutchinson, J.B., Uncapher, M.R., and Wagner, A.D. (2015). Increased functional connectivity between dorsal posterior parietal and ventral occipitotemporal cortex during uncertain memory decisions. *Neurobiol. Learn. Mem.* *117*, 71–83.
- Insausti, R., and Muñoz, M. (2001). Cortical projections of the non-entorhinal hippocampal formation in the cynomolgus monkey (*Macaca fascicularis*). *Eur. J. Neurosci.* *14*, 435–451.
- Kahana, M.J. (2012). *Foundations of Human Memory* (Oxford University Press).
- Kiani, R., and Shadlen, M.N. (2009). Representation of confidence associated with a decision by neurons in the parietal cortex. *Science* *324*, 759–764.
- Klaes, C., Kellis, S., Afalalo, T., Lee, B., Pejisa, K., Shanfield, K., Hayes-Jackson, S., Aisen, M., Heck, C., Liu, C., and Andersen, R.A. (2015). Hand shape representations in the human posterior parietal cortex. *J. Neurosci.* *35*, 15466–15476.
- Kwon, S.E., Yang, H., Minamisawa, G., and O'Connor, D.H. (2016). Sensory and decision-related activity propagate in a cortical feedback loop during touch perception. *Nat. Neurosci.* *19*, 1243–1249.
- Lavenex, P., Suzuki, W.A., and Amaral, D.G. (2002). Perirhinal and parahippocampal cortices of the macaque monkey: projections to the neocortex. *J. Comp. Neurol.* *447*, 394–420.
- Manns, J.R., Hopkins, R.O., Reed, J.M., Kitchener, E.G., and Squire, L.R. (2003). Recognition memory and the human hippocampus. *Neuron* *37*, 171–180.
- Metcalfe, J. (2008). Metamemory. In *Learning and Memory: A Comprehensive Reference* H. L. Roediger, ed. (Elsevier), pp. 349–362.
- Nelson, S.M., Cohen, A.L., Power, J.D., Wig, G.S., Miezin, F.M., Wheeler, M.E., Velanova, K., Donaldson, D.I., Phillips, J.S., Schlaggar, B.L., and Petersen, S.E. (2010). A parcellation scheme for human left lateral parietal cortex. *Neuron* *67*, 156–170.
- Nelson, S.M., McDermott, K.B., Wig, G.S., Schlaggar, B.L., and Petersen, S.E. (2013). The critical roles of localization and physiology for understanding parietal contributions to memory retrieval. *Neuroscientist* *19*, 578–591.
- Nieder, A., and Miller, E.K. (2004). A parieto-frontal network for visual numerical information in the monkey. *Proc. Natl. Acad. Sci. USA* *101*, 7457–7462.
- Olson, I.R., and Berryhill, M. (2009). Some surprising findings on the involvement of the parietal lobe in human memory. *Neurobiol. Learn. Mem.* *91*, 155–165.
- Pouzat, C., Mazor, O., and Laurent, G. (2002). Using noise signature to optimize spike-sorting and to assess neuronal classification quality. *J. Neurosci. Methods* *122*, 43–57.
- Raposo, D., Kaufman, M.T., and Churchland, A.K. (2014). A category-free neural population supports evolving demands during decision-making. *Nat. Neurosci.* *17*, 1784–1792.
- Rishel, C.A., Huang, G., and Freedman, D.J. (2013). Independent category and spatial encoding in parietal cortex. *Neuron* *77*, 969–979.
- Rugg, M.D., and Curran, T. (2007). Event-related potentials and recognition memory. *Trends Cogn. Sci.* *11*, 251–257.
- Rugg, M.D., and King, D.R. (2017). Ventral lateral parietal cortex and episodic memory retrieval. *Cortex*. Published online July 25, 2017. <https://doi.org/10.1016/j.cortex.2017.07.012>.
- Rutishauser, U., Schuman, E.M., and Mamelak, A.N. (2006). Online detection and sorting of extracellularly recorded action potentials in human medial temporal lobe recordings, in vivo. *J. Neurosci. Methods* *154*, 204–224.
- Rutishauser, U., Schuman, E.M., and Mamelak, A.N. (2008). Activity of human hippocampal and amygdala neurons during retrieval of declarative memories. *Proc. Natl. Acad. Sci. USA* *105*, 329–334.
- Rutishauser, U., Ye, S., Koroma, M., Tudusciuc, O., Ross, I.B., Chung, J.M., and Mamelak, A.N. (2015). Representation of retrieval confidence by single neurons in the human medial temporal lobe. *Nat. Neurosci.* *18*, 1041–1050.
- Sestieri, C., Shulman, G.L., and Corbetta, M. (2010). Attention to memory and the environment: functional specialization and dynamic competition in human posterior parietal cortex. *J. Neurosci.* *30*, 8445–8456.
- Sestieri, C., Tosoni, A., Mignogna, V., McAvoy, M.P., Shulman, G.L., Corbetta, M., and Romani, G.L. (2014). Memory accumulation mechanisms in human cortex are independent of motor intentions. *J. Neurosci.* *34*, 6993–7006.
- Sestieri, C., Shulman, G.L., and Corbetta, M. (2017). The contribution of the human posterior parietal cortex to episodic memory. *Nat. Rev. Neurosci.* *18*, 183–192.
- Shadlen, M.N., and Newsome, W.T. (2001). Neural basis of a perceptual decision in the parietal cortex (area LIP) of the rhesus monkey. *J. Neurophysiol.* *86*, 1916–1936.
- Shannon, B.J., and Buckner, R.L. (2004). Functional-anatomic correlates of memory retrieval that suggest nontraditional processing roles for multiple distinct regions within posterior parietal cortex. *J. Neurosci.* *24*, 10084–10092.
- Simons, J.S., Peers, P.V., Mazuz, Y.S., Berryhill, M.E., and Olson, I.R. (2010). Dissociation between memory accuracy and memory confidence following bilateral parietal lesions. *Cereb. Cortex* *20*, 479–485.
- Uddin, L.Q., Supekar, K., Amin, H., Rykhlevskaia, E., Nguyen, D.A., Greicius, M.D., and Menon, V. (2010). Dissociable connectivity within human angular gyrus and intraparietal sulcus: evidence from functional and structural connectivity. *Cereb. Cortex* *20*, 2636–2646.
- Uncapher, M.R., and Wagner, A.D. (2009). Posterior parietal cortex and episodic encoding: insights from fMRI subsequent memory effects and dual-attention theory. *Neurobiol. Learn. Mem.* *91*, 139–154.
- Vilberg, K.L., and Rugg, M.D. (2008). Memory retrieval and the parietal cortex: a review of evidence from a dual-process perspective. *Neuropsychologia* *46*, 1787–1799.
- Wagner, A.D., Shannon, B.J., Kahn, I., and Buckner, R.L. (2005). Parietal lobe contributions to episodic memory retrieval. *Trends Cogn. Sci.* *9*, 445–453.
- Wheeler, M.E., and Buckner, R.L. (2003). Functional dissociation among components of remembering: control, perceived oldness, and content. *J. Neurosci.* *23*, 3869–3880.
- Wimber, M., Rutschmann, R.M., Greenlee, M.W., and Bäuml, K.H. (2009). Retrieval from episodic memory: neural mechanisms of interference resolution. *J. Cogn. Neurosci.* *21*, 538–549.
- Wixted, J.T. (2007). Dual-process theory and signal-detection theory of recognition memory. *Psychol. Rev.* *114*, 152–176.
- Wixted, J.T., Mickes, L., and Squire, L.R. (2010). Measuring recollection and familiarity in the medial temporal lobe. *Hippocampus* *20*, 1195–1205.
- Yassa, M.A., and Stark, C.E. (2008). Multiple signals of recognition memory in the medial temporal lobe. *Hippocampus* *18*, 945–954.
- Yonelinas, A.P., Otten, L.J., Shaw, K.N., and Rugg, M.D. (2005). Separating the brain regions involved in recollection and familiarity in recognition memory. *J. Neurosci.* *25*, 3002–3008.
- Zhang, C.Y., Afalalo, T., Revechikis, B., Rosario, E.R., Ouellette, D., Pouratian, N., and Andersen, R.A. (2017). Partially mixed selectivity in human posterior parietal association cortex. *Neuron* *95*, 697–708.e4.

STAR★METHODS

KEY RESOURCES TABLE

| REAGENT OR RESOURCE | SOURCE | IDENTIFIER |
|--|------------------------|---|
| Software and Algorithms | | |
| MATLAB R2016a | MathWorks | RRID: SCR_001622; https://www.mathworks.com |
| OSort | N/A | RRID: SCR_015869; http://www.rutishauserlab.org/osort |
| Psychophysics toolbox PTB3 | N/A | RRID: SCR_002881; http://psychtoolbox.org |
| Other | | |
| Neuroport Recording System, Utah array implant | Blackrock Microsystems | http://blackrockmicro.com |

CONTACT FOR REAGENT AND RESOURCE SHARING

Further information and requests for resources should be directed to the Lead Contact, Ueli Rutishauser (urut@caltech.edu).

EXPERIMENTAL MODEL AND SUBJECT DETAILS

Two tetraplegic subjects (NS and EGS; NS is female, age 59; EGS is male, age 36) chronically implanted with a 96-channel Utah electrode array in the IPPC took part in the study. Both subjects were enrolled in an ongoing BMI study, as part of which they had already consented to the surgical procedure. We received FDA IDE clearance (IDE #G120096, G120287) to extend the duration of the implant for the purpose of our ongoing clinical study. This study was approved by the institutional review boards of the California Institute of Technology, UCLA, and Casa Colina Centers for Rehabilitation.

METHOD DETAILS

Memory Task

The experiment consisted of two separate blocks: a learning block, followed by a recognition block. Each image belonged to one of five visual categories, such as animals, people, food items, places, and objects. All images were initially novel, i.e., for each testing session a new set of images were used (Table S1). Thus, novel images were truly novel because each was seen for the very first time by the subject. During the learning block, subjects viewed 75-100 novel (never seen before) and unique images. After each image, subjects were asked whether the image contained an animal (yes/no). After a delay of on average 36min length (see Table S1), subjects then performed the recognition block. Subjects were shown the original 75-100 images seen during learning (now familiar) randomly intermixed with an equal number of novel images (total 150-200 trials). Each image was displayed for 1 s, followed by a delay period lasting 1.1-1.6 s (randomized). At the end of the delay period, the question screen appeared prompting subjects to indicate with a verbal response (1-6 confidence scale) whether they thought they had seen the image before or not (old or new) and how confident they were of their decision. Subjects were instructed to use the following response mapping: 1 = new confident, 2 = new probably, 3 = new guessing, 4 = old guessing, 5 = old probably, 6 = old confident. The experimenter entered a number between 1 and 6 as soon as it was possible to determine which number was spoken by the subject. Subjects were asked to only respond by saying a single number (1-6) and to only respond after onset of the response screen. No trial-by-trial feedback was provided. The task was implemented in MATLAB using Psychophysics toolbox (Brainard, 1997). Subjects sat in a motorized wheel chair in front of a 27inch LCD monitor occupying approximately 40 degrees of visual angle.

Control Task

The experiment was identical to the recognition block of the memory task, except that the images were replaced with a randomly chosen number in the range of 1-6. Subjects were instructed to remember the number and provide it as an answer after the question screen. Each session of the control task consisted of 60 trials.

Electrode Placement and Electrophysiology

Arrays were targeted to the putative human homolog of macaque area AIP as identified using a previous fMRI study (Aflalo et al., 2015). The electrode locations were (−36, −48, 53) and (−38, −53, 46) for NS and EGS, respectively (Tailarach coordinates). Details on EGS have been published before (Aflalo et al., 2015). Similarly, details on NS have been published before (Zhang et al., 2017). Neural activity was amplified, digitized at 30kHz, and recorded with a Blackrock Neuroport system as described before (Aflalo et al., 2015).

QUANTIFICATION AND STATISTICAL ANALYSIS

Spike Detection and Sorting

The raw signal was filtered with a zero-phase lag filter in the 300–3000 Hz band and spikes were then detected and sorted with the semiautomatic template matching algorithm ‘OSort’ as previously described (Rutishauser et al., 2006). We used rigorous metrics to quantify spike sorting quality and to identify putative single units. Criteria that we used (see Figure S1 for actual values) were: i) percentage of interspike intervals (ISIs) shorter than 3ms, ii) signal-to-noise (SNR) of the mean waveform, iii) pairwise projection distance in clustering space (Pouzat et al., 2002), iv) modified coefficient of variation of the ISI (CV2), and v) isolation distance (Harris et al., 2000) of each cluster versus all other spikes detected on that same channel. We treated neurons recorded on different days as different neurons. Recording sessions were spaced out by multiple weeks to increase the chances that neurons recorded on the same channel differed between sessions.

Behavioral Analysis

For the decision time we used the time that elapsed between question onset and onset of speech, as marked by an experimenter. Each recognition trial was categorized into one of four categories: true positive (old stimulus rated as 4–6), true negative (new stimulus rated as 1–3), false positive (new stimulus rates as 4–6), and false negative (old stimulus rated as 1–3). We pooled medium (2 or 5) and guessing level (3 and 4) confidence trials together as “low confidence” trials for all analysis except where noted (analysis that involves the “medium” rating is not pooled). We used a 2x2 repeated-measure ANOVA with fixed factors familiarity (new/old) and confidence (high/low) and random factor session ID to assess the relationship between behavior, memory, and decision time.

Single-Neuron Analysis

We used the firing rate in a 2 s window starting 200ms after stimulus onset to select neurons and perform single-neuron ROC analysis. We did not use the first 200ms after stimulus onset because none of the neurons responded in this early period and to maintain consistency with earlier work. MS neurons were selected if the mean firing rate between new and old trials that were correctly identified by the subject (regardless of confidence) differed significantly ($p < 0.05$, two-tailed, bootstrap comparison of means with 1000 runs). Note that this selection does not have access to the confidence of the choice, making this variable statistically independent after selecting cells (see Figure S4 for a test of this assertion). Confidence-coding neurons were identified by comparing high- and low confidence trials (regardless if new or old) for correct trials only ($p < 0.05$, two-tailed, bootstrap comparison of means with 1000 runs). For all PSTH plots, we used non-overlapping bins of 250ms width. For plotting purposes only, single-neuron PSTH diagrams were smoothed with a Gaussian kernel of 200ms s.d. Normalized firing rates were estimated by dividing the response by the average overall firing rate of a neuron throughout the entire experiment.

Single-Neuron ROC Analysis

We used ROC analysis to quantify how well the activity of a single neuron differentiated between two conditions. We summarized each ROC by its area under the curve (AUC). Based on the AUC, we then defined a neurons preference index as $2*(AUC-0.5)$ (Raposo et al., 2014). For MS and CS neurons, we refer to this preference index as ‘memory preference’ and ‘confidence preference’, respectively. Preference index values varied between $-1 \dots 1$. For ‘memory preference’, we assessed whether old $>$ new and for ‘confidence preference’ whether high $>$ low. Positive preference index values thus indicate higher firing rates for old and high confidence trials, respectively. Negative preference index values, on the other hand, indicate higher firing rates for new and low confidence trials, respectively. We counted spikes in a 2 s window starting 200ms after stimulus onset for all ROC analysis, with the exception of time courses, where we used a 500ms time window moved in steps of 100ms.

Independence of Cell Selection and ROC Analysis Bootstrap

For each bootstrap run (executed 1000 times), we selected a random subset of 50% of the trials for each session for cell selection and used the remaining 50% of the trials to perform the single-neuron ROC analysis (see above). For each run, we then averaged the observed AUC for high- and low confidence trials and the confidence preference index for all selected MS and CS cells. These AUC values were computed based only on the test trials not used for selection. For chance controls, we randomly scrambled the order of the responses given and the ground truth labels. Otherwise, everything was identical.

Choice and Memory Probability Analysis

The choice probability (CP) of a neuron is equal to the AUC of a neuron when comparing new versus old choices regardless of whether they were correct or incorrect. Similarly, the memory probability (MP) is equal to the AUC of a neuron when comparing stimuli according to their ground truth (new versus old), regardless of the decision made by the subject. This strategy is similar to that used previous in comparing choice- and sensory probability (Kwon et al., 2016). To compare CP as a function of confidence across the population, we used a repeated-measure 1x3 ANOVA with cell ID as a random factor and confidence (high, medium, low) as a fixed factor and CP as the predictor.

Population Analysis

We used a series of mixed-effect generalized linear models (GLM) to further analyze groups of selected cells. Only correct trials were included. As fixed effects we used subsets of familiarity (New or old), confidence (high or low) and decision time (DT, in seconds). Familiarity and confidence were categorical variables. All models listed below include as random effects cell ID nested within session ID. To assess the effect of interactions between confidence and familiarity, we compared model 1 (Fixed effects familiarity and confidence) with model 2 (model 1 plus an interaction term between familiarity and confidence). To assess the effects of DT, we in addition added the fixed effect DT to model 1 and 2 and then compared the two. Model comparisons were performed based on the Akaike information criterion (AIC), expressed as a log likelihood ratio. GLM models were fit and compared using the MATLAB functions 'fitglm' and 'compare', respectively. The link function was poisson.

Decoding

We used a regularized least-square decoder as previously described (Rutishauser et al., 2008). We trained on 60% of all available trials and tested on the remaining 40%. The 60/40 split was randomized and decoding performance was averaged across 10 bootstrap runs. We trained one decoder for each session, i.e., the decoder had access to all simultaneously recorded neurons. Only correct trials were used for all decoding analysis.

Latency Analysis

Latency was estimated based on the cumulative sum of the spike train as previously described (Rutishauser et al., 2015). For each neuron, we first computed the cumulative sum of each trial in 1ms steps. We then averaged the cumulative sums of all trials of the preferred and the non-preferred stimulus type of each MS cell and then averaged the preferred-and non-preferred average cumulative sums across cells. To estimate the first point of time where the two cumulative sums diverged, we performed a paired t test at every point of time ($p < 0.05$). The latency was defined as the first point of time after which this comparison remains significant. Note that due to the pairwise test, this method is not sensitive to differences in baseline firing rates.

Bootstrap Statistics

Bootstrap statistics were run with $B = 1000$ iterations. We used $p = 1/B$ in cases where no example of the null distribution exceeded the observed value.

DATA AND SOFTWARE AVAILABILITY

The spike detection and sorting toolbox OSort was used for data processing, which is available as open source. Data and custom MATLAB analysis scripts are available upon reasonable request from Ueli Rutishauser (urut@caltech.edu).

ADDITIONAL RESOURCES

This study was conducted as part of NIH clinical trial NCT01958086.